

Influence of Fe₃O₄ particles in Al7075 metal matrix composites: A Tribological study

A. Shivaramakrishna, Raghavendra Subramanya, Yadavalli Basavaraj, R. Arun Kumar,
M. Ravi Kumar, N. Kiran Kumar, R. Suresh

Due to their widespread use in the automotive and aerospace industries, among many other engineering applications, aluminum metal-matrix composites are attracting a lot of research interest. Its low wear rate and excellent strength make it the favored alternative. The main objective of this research project is to create metal-matrix composite materials by utilizing Fe₃O₄ as a reinforcing element and aluminum alloy 7075 as the matrix material. This study examined the dry sliding wear behavior of Al7075 alloy reinforced with varying weight proportions (3%, 6%, and 9%) of Fe₃O₄ (Magnetite) on composite samples using a pin-on disc apparatus. The composite was maintained unlubricated, and the volumetric wear rate by the pin-on disc wear machine in moist air was measured. The sliding speeds ranged from 1 to 3 m/s for a constant sliding distance of 1500 meters. The coefficient of friction decreased as the reinforcement percentage of Fe₃O₄ increased in the aluminum matrix, and also, volumetric wear loss increased as the load increased. The wear tests were carried out using the Taguchi orthogonal approach for reducing the trials of the experiments and to optimize the wear rate and frictional force of Al7075-Fe₃O₄ composite. A mathematical model was obtained to determine the wear rate and frictional force of Al7075-Fe₃O₄ composite.

Introduction



Particulate-reinforced Metal Matrix Composites (MMCs), which are composed of hard ceramic particles embedded in a ductile metallic matrix, have gained significant interest because of their superior mechanical and tribological qualities when compared to traditional alloys [1]. While retaining a relatively low density, the use of ceramic reinforcements like Al₂O₃, SiC, TiC, and Fe₃O₄ greatly enhances characteristics like wear resistance, specific strength, stiffness, and thermal stability [2]. These features make MMCs particularly suitable for aerospace and automotive applications, where components must sustain high mechanical loads, frictional contact, and elevated operating temperatures without excessive wear or deformation. Ceramic reinforcements considerably boost the strength and rigidity of the composite while keeping the weight low. Used in high-temperature, high-friction components such as pistons, cylinder liners, braking rotors/drums, and connecting rods in automobiles. In contrast, Metal matrix composites are used to develop landing gear components, helicopter rotor blade sleeves, and structural struts in spacecraft [3].


Wear is defined as the progressive removal of material from a surface caused by mechanical interaction with another in relative motion, remains a major limitation to the service life of engineering components. Proper selection is required as the type, nature, shape, and size of reinforcements have a significant impact on how well aluminum matrix composites wear. It is clear from the literature that any aluminum base alloys' wear rates increased when sliding speed, sliding distance, and applied load increased. Nonetheless, the hybridized composite showed superior wear resistance, most likely as a result of the ceramic particle reinforcements. The particles reduced the rate at which material was being removed from the composite's surface by offering a significant degree of resistance to the abrasive's micro cutting of the composite.


Additionally, the investigations revealed that when the load increased, the rate of wear increased for both the composite and the aluminum alloy. However, when


reinforcement was included, the wear mechanism abruptly shifted from mild to severe wear, resulting in a faster rate of material loss of the base alloy. The ceramic reinforcement in the composite samples caused their transition values to be delayed.


To enhance the wear resistance of aluminum-based materials, numerous studies have examined the influence of processing parameters and reinforcement characteristics under dry sliding conditions [4]. These works generally demonstrate that wear behavior is strongly affected by factors such as reinforcement type, weight fraction, sliding speed,


A. Shivaramakrishna , Yadavalli Basavaraj 
*Department of Mechanical Engineering,
Ballari Institute of Technology and Management
Ballari, Karnataka, 583 104, India.*

Raghavendra Subramanya 
*Department of Mechanical Engineering,
Sai Vidya Institute of Technology
Bangalore, Karnataka, 560 064, India.*

R. Arun Kumar 
*Department of Mathematics, Sai Vidya Institute of Technology
Bangalore, Karnataka, 560 064, India.*

M. Ravi Kumar 
*Department of Mechanical Engineering,
BMS college of Engineering
Bangalore, Karnataka, 560 019, India.*

N. Kiran Kumar 
*Department of Mechanical Engineering,
Vemana Institute of Technology
Bangalore, Karnataka, 560 034, India*

R. Suresh 
*Department of Mechanical Engineering,
M.S. Ramaiah University of Applied Sciences
Bangalore, Karnataka, 560 054, India*

Received: August 26th, 2025.

Accepted: January 27th, 2026.

Published: March 9th, 2026.

© 2026 by the authors. Creative Commons Attribution
https://doi.org/10.47566/2026_syv39_1-260301

applied load, and counter-face hardness, which collectively determine the stability of the tribo-layer and the rate of material loss.

Sahin [5] reported that increasing the iron content in aluminum-based composites resulted in a reduction in wear rate across a broad range of applied loads and sliding velocities, owing to the formation of a harder surface layer and improved load-bearing capacity. Similarly, Mondal *et al.* [6] found that the addition of iron oxide (Fe_3O_4) particles to cast aluminum alloys improved both mechanical strength and wear resistance. Their study attributed these improvements to dispersion hardening and the development of a protective oxide film during sliding, which minimized adhesive wear and surface damage.

The beneficial effects of hard reinforcements – whether in the form of particles, fibers, or whiskers – on MMCs have also been well documented [7]. These phases enhance the tribological performance by increasing surface hardness, reducing adhesion, and stabilizing tribo-oxide films that protect the sliding interface. Consequently, such composites are considered promising candidates for applications involving sustained sliding or abrasive contact, where their combination of high specific strength, wear resistance, and good thermal conductivity offers significant performance advantages [8].

The influence of critical parameters – such as reinforcement volume fraction and particle size, sliding speed, applied load, and counter-face hardness – on the dry sliding wear behavior of aluminum-based MMCs has been comprehensively investigated in prior research. For instance, Gopalsamy *et al.* [9] studied the two-body abrasive wear behavior of aluminum alloy reinforced with 10 wt% Al_2O_3 particles and demonstrated that wear resistance increased with higher applied load and smaller abrasive particle size. Their statistical analysis also revealed significant interactions between reinforcement content and applied load, indicating the complex interplay between microstructural features and operating conditions.

To systematically identify and optimize such influences, several researchers have employed design of experiments (DoE) techniques, including the Taguchi method, Response Surface Methodology (RSM), Full Factorial Design, and Analysis of Variance (ANOVA) [10–12]. These approaches enable quantitative evaluation of factor significance, model development for wear prediction, and optimization of processing and testing conditions to enhance composite performance.

Despite extensive studies on aluminum-based MMCs, relatively few investigations have focused on Fe_3O_4 -reinforced Al7075 composites. The present study aims to address this gap by fabricating Al7075- Fe_3O_4 composites using the stir casting method and evaluating their dry sliding wear performance through pin-on-disc experiments. The effects of three parameters, reinforcement percentage (3, 6, and 9 wt%), applied load, and sliding speed, were analyzed using the Taguchi orthogonal array design, followed by statistical validation using ANOVA. This research establishes a systematic relationship between Fe_3O_4 reinforcement and wear behavior in Al7075 matrices,

Table 1. Chemical composition of Al7075.

Element	Content (wt%)
Si	0.4
Mn	0.3
Zn	6.1
Cu	2
Ti	0.2
Mg	2.9
Cr	0.28
Al	Balance

contributing to the broader understanding of wear-resistant MMC development for engineering applications.

Materials and Methods

Specimen Preparation

Al7075 alloy was used as the matrix material, and magnetite (Fe_3O_4 , 300 mesh) served as the particulate reinforcement. Composite castings were produced by the stir-casting route. In a typical run, Al7075 billets were placed in a graphite crucible and melted in a muffle furnace at ≈ 660 °C. Fe_3O_4 powder was preheated to 250 °C for 1 h to remove adsorbed moisture, then introduced slowly into the molten aluminum while stirring. Mechanical stirring was performed at 400 rpm for 6–8 minutes to enhance wetting and obtain a near-uniform dispersion of particles. The molten composite was then poured into a preheated steel mold (die) and allowed to cool to room temperature [9]. After solidification, castings were removed, machined and turned to produce pins of 10 mm diameter \times 50 mm length for pin-on-disc wear testing. Specimens were degreased in acetone and oven-dried before testing.

The Fe_3O_4 reinforcement content investigated was 3, 6, and 9 wt%. Particle size was 300-mesh (nominal mean size ≈ 45 μm). The chemical composition of the Al7075 parent alloy was obtained from the material certificate supplied by the vendor (Table 1).

Dry sliding wear test

Dry sliding wear experiments were performed on a DUCOM pin-on-disc tribometer (model TR-20 or equivalent). A labelled schematic of the test rig is provided, and a photograph is shown in Figure 1. The schematic illustrates the pin clamping, the rotating disc, the load application mechanism, and the locations of the friction and displacement sensors. The tribometer applies the normal load through a calibrated loading arm and load cell; the friction force is recorded continuously by the friction transducer and logged by the wear monitor (the “wear monitor” records real-time friction force and computes the coefficient of friction (COF) as $\mu = \text{friction force} / \text{normal load}$).

As shown in Figure 2 pins were machined to 10.0 ± 0.05 mm diameter and 50.0 ± 0.2 mm length from the cast

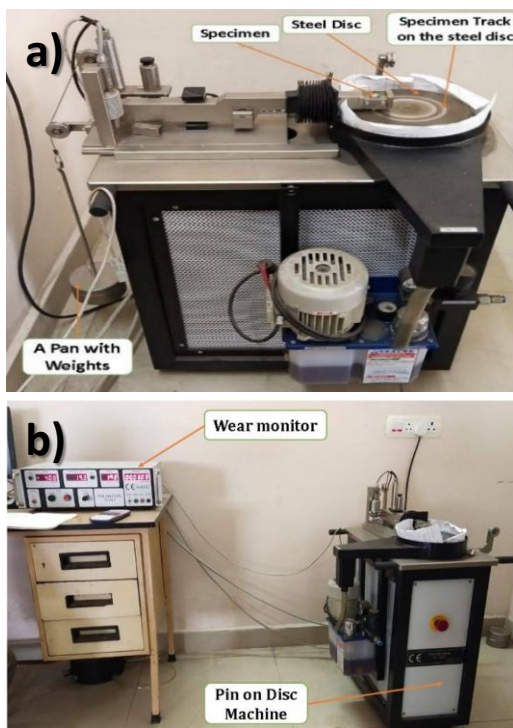


Figure 1. Pin-on Disc wear machine (a) showing: rotating disc, pin holder, and indicated track diameter (100 mm) (b) data logger (wear monitor).

billets. EN32 steel discs (hardened and ground) were used as counter faces; disc hardness and surface finish were measured before testing (EN32, HRC ≈ 58; Ra ≈ 0.20 μm). To maintain comparable contact conditions across the L9 test matrix, the same disc was reused during the experimental campaign and refurbished between selected runs (light polishing/turning and ultrasonic cleaning) to remove adherent debris and restore a consistent surface finish. If a disc showed excessive scoring or embedded debris, it was replaced. The manuscript’s final version should state whether discs were replaced after X runs (insert your lab practice here).

The test matrix used a Taguchi L9 orthogonal array with three factors and three levels: reinforcement (3, 6, 9 wt% Fe₃O₄), applied load (10, 30, 50 N) and sliding speed (0.5, 1.0, 1.5 m/s). The track diameter was 100 mm; the selected rotational speeds produced the above linear sliding velocities. Each test was run for a fixed sliding distance of 1500 m or until seizure; the machine recorded friction continuously to produce COF vs. sliding distance curves.

Before testing, pin specimens were degreased in acetone, ultrasonically cleaned for 5 min, and oven-dried. Pins were



Figure 2. Wear test specimens of Al-Fe₃O₄ composites with varying reinforcement contents (3%, 6%, and 9% Fe₃O₄).

weighed before and after each test on an electronic microbalance (accuracy ±0.01 mg). Mass loss (Δm) was converted to volumetric wear rate (VWR, mm³·m⁻¹) using the specimen density (ρ) and the test sliding distance (L) as:

$$VWR = (\Delta m / \rho) / L \text{ (mm}^3\text{m}^{-1}\text{)}$$

All tests were repeated at least twice; mean values are reported. The COF was calculated from the recorded friction force and the applied normal load; steady-state COF values were obtained by averaging the recorded COF over the steady portion of the run (after the running-in transient).

Taguchi and statistical measurement details (methods). The Taguchi L9 design reduces the experimental burden while permitting main-effect estimation. For each run the “smaller-is-better” signal-to-noise (S/N) ratio for VWR was computed as:

$$S/N = -10 \cdot \log_{10} \left[(1/n) \sum (y_i)^2 \right]$$

where y_i are replicate VWR values and n is the number of replicates. ANOVA (95% confidence) was used to quantify factor contributions and test significance (p < 0.05). Model fitting and confirmation runs were performed to validate the regression equations derived from the Taguchi data.

Surface and microstructural characterization (methods). After wear testing, representative pin specimens were sectioned and the worn surfaces examined using scanning electron microscopy (FE-SEM: ELIONIX, ERA-8800FE) at 15 kV to identify dominant wear features (grooves, particle pull-out, delamination, oxide film). Non-conductive samples were sputter-coated with ~5 nm of Au/Pd before imaging. Energy dispersive X-ray spectroscopy (EDS) was carried out on selected regions to detect Fe- and O-rich tribo-films and to confirm the presence of Fe₃O₄ in the debris.

Results and discussion

Wear behavior

Figure 3 shows the Coefficient of Friction (COF) curves for the composite sample under different applied load configurations. The Coefficient of Friction (COF) value was lower at high loads. The reduction of the coefficient is associated with the slow formation of a surface oxide layer that grows with temperature under increasing pressure strains on the contacts.

Variation of Coefficient of Friction with sliding distance under a load of 10 N, 30 N, 50 N, and speed of (a) 0.5 m/s, (b) 1 m/s, and (c) 1.5 m/s for Casted Al-3wt% iron oxide, Al-6wt% iron oxide, and Al-9wt% iron oxide, respectively.

From the above graphs, COF decreases with increasing loads for Al-9wt% iron oxide, and in some above cases, COF increases with increasing loads at different speeds.

The residual oxide layer acts as a surface for lubrication. The research suggests that the decrease in the coefficient is due to the thickening of the oxide layer that develops in systems where oxidation is a significant factor in the wear process [10-11]. The COF increases as the applied stress increases. Friction between the contacts may cause dirt and ceramic pieces to detach from the layer, leading to increased wear by abrasion.

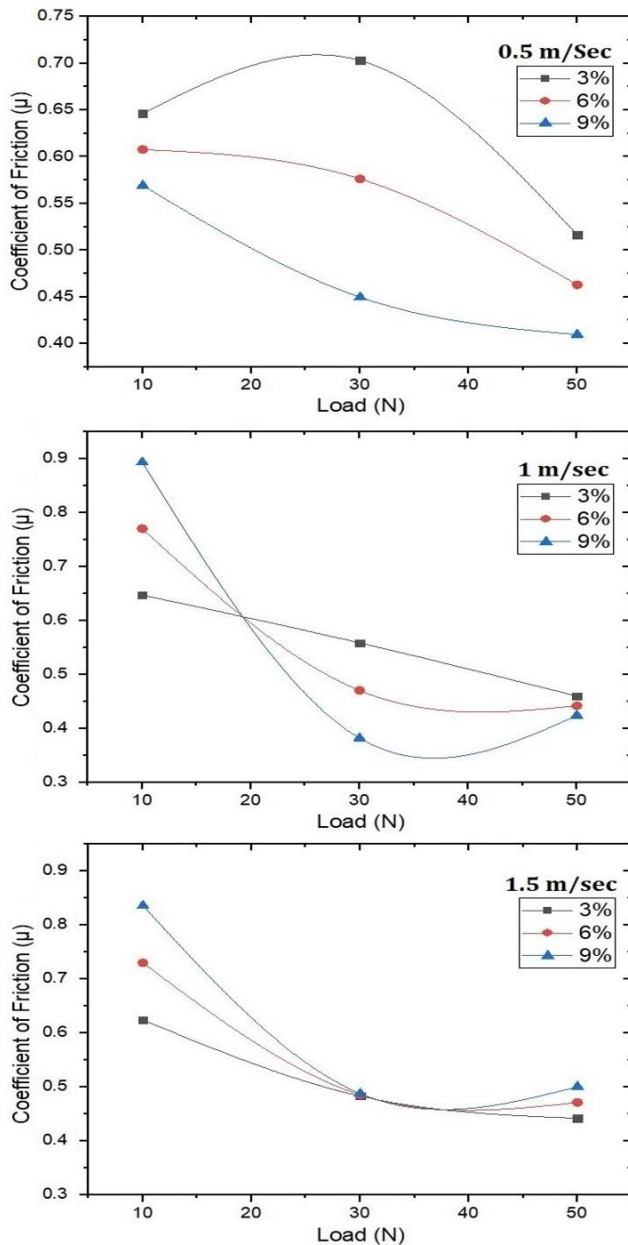


Figure 3. Effect of load on the Coefficient of friction of AMC at various speeds of (a) 0.5m/s, (b) 1 m/s and (c) 1.5 m/s.

At varying normal loads, the COF of the aluminum-reinforced iron oxide composite sample drops somewhat as sliding speeds increase. It was evident that the coefficient of friction is only significantly impacted by sliding speed at lower sliding speeds. Furthermore, compared to the effect of normal load on the coefficient of friction, the influence of sliding speed on the latter is less substantial. The wear rate increases more quickly when the load is raised. This leads to a rougher MMC surface and larger wear detritus. There is a second transition from severe wear to sliding wear as the load is increased further. Work hardening and the rapid oxidation of the surface material are most likely to blame for this. Because the load increases the surface temperature, the specimen surface oxidizes more. Surface oxidation was indicated by darker patches on the surface and a consistent increase in hardness with increasing pressure. It has been

discovered that a metal oxide coating improves the wear resistance of MMCs [12].

Because of ploughing between the pin and disc, more debris projects from the pin surface at higher normal loads. Consequently, the debris layer reduces the direct contact between the sample and disc surfaces, which in turn lowers the COF.

Variation of Volumetric Wear Rate (mm^3/m) with Load (N) for Al-3%, 6% and 9% iron oxide at 0.5 m/s, 1 m/s, and 1.5 m/s Sliding speeds are shown in Figure 4.

It was observed that the volumetric wear rate was increased with an increase in the Load (10 N, 30 N, 50 N) at 0.5 m/s, 1 m/s, and 1.5 m/s. Also, the VWR slightly increases with up to 30 N thereafter decreases with 50 N due to formation of Oxide layer for 0.5 m/s, VWR is initially slightly increasing at lower loads (10 N and 30 N) and increases with higher loads (50 N) for 1 m/s, VWR increases at lower loads and

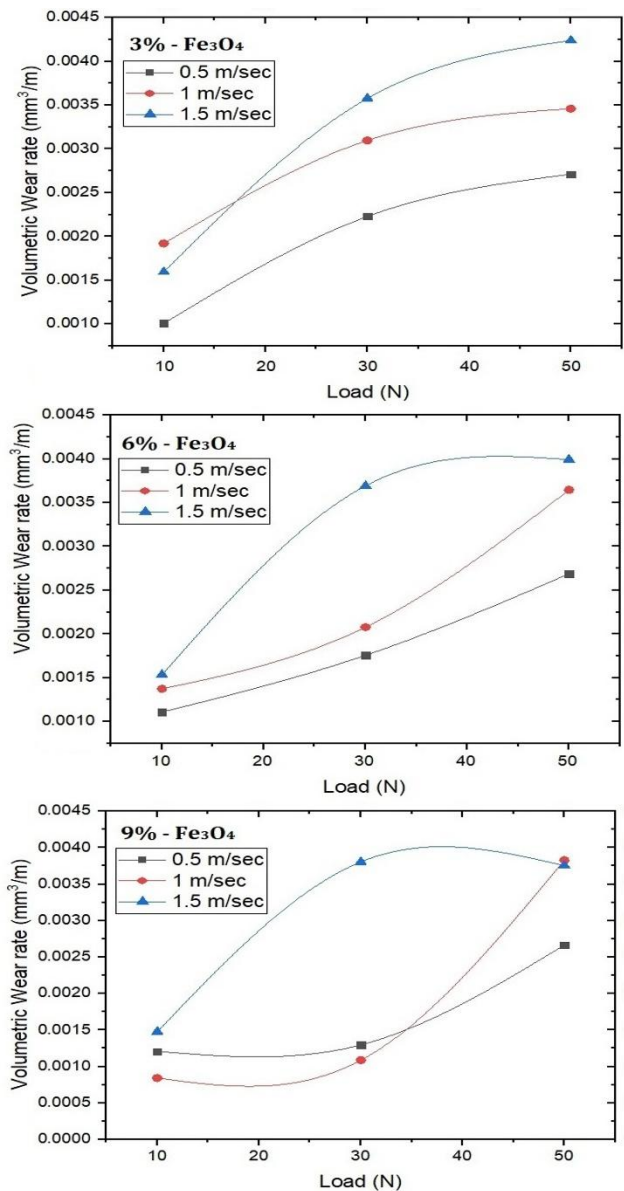


Figure 4. Effect of volumetric wear Rate (VWR) Cast Composite on different loads at different speeds of (a) 3%, (b) 6%, and (c) 9% reinforcement.

Table 2. Control Factors and Their Levels.

Control Factors	Level			Units
	1	2	3	
Reinforcement (A)	3	6	9	wt%
Applied Load (B)	10	30	50	N
Sliding Speed (C)	0.5	1.0	1.5	m/s

again increases at higher loads, at 50 N decreases VWR due to friction for 1.5 m/s.

Friction increases in proportion to the load. These findings align with the findings of Chowdhury and Khalil [13] for aluminum and, more broadly, for surfaces that include metal oxide, dampness, etc. The aluminum-silicon casting alloy readily oxidises in the air within the first few minutes of friction. As the load grows, the metal deteriorates and wears out more. In the initial rubbing phase, the surface layers are broken, the surfaces are cleaned and smoothed, and the connections and contact between them are strengthened. Because of the friction force brought on by the tillage action, the temperature between the surface’s increases. This process generates adhesion and enhances surface layer deformation, which progressively reduces the metal.

A change in shear rate leads to a shift in sliding speed and increased load, which in turn causes a low coefficient of friction. Adhesion results from this phenomenon's effects on the mechanical properties of materials, which include increased surface wear and degradation, decreased contact area, and oxide layer fracture. The amount of wear from one stage to the next is determined by the test parameters, and the sliding speed results in the growth of a thin film protector, which decreases surface contact and validates the results of Alias and Hague [14].

Taguchi approach

The purpose of the studies is to examine how testing factors affected the particular wear rate of Al7075 composite (Reinforced by 3%, 6%, and 9% weight). Table 2 displays the code and control parameter levels. This demonstrates the three tiers of the experimental plan.

Table 3. Wear test details of Al7075 + 3%, 6%, and 9% iron oxide Specimen for 0.5, 1.0, and 1.5 m/s using Taguchi L9 array.

Reinforcement (wt%)	Applied load (N)	Sliding speed (m/s)	VWR (mm ³ /m)	SNRA1
3	10	0.5	0.00101	59.91357
3	30	1	0.0031	50.17277
3	50	1.5	0.00424	47.45268
6	10	1	0.00137	57.26559
6	30	1.5	0.00369	48.65947
6	50	0.5	0.00269	51.40495
9	10	1.5	0.00148	56.59477
9	30	0.5	0.0013	57.72113
9	50	1	0.00383	48.33602

Table 4. Response Table for Signal-to-Noise Ratios: Smaller is better.

Level	Reinforcements (wt%)	Applied load (N)	Sliding Speed (m/s)
1	52.51	57.92	56.35
2	52.44	52.18	51.92
3	54.22	49.06	50.90
Delta	1.77	8.86	5.44
Rank	3	1	2

Delta: difference between the maximum and minimum mean values for each factor.
Rank: order of influence of the factors on the response variable.

Table 5. Response Table for Means for VWR (mm³/m).

Level	Reinforcement	Applied load	Sliding Speed
1	0.002783	0.001287	0.001667
2	0.002583	0.002697	0.002767
3	0.002203	0.003587	0.003137
Delta	0.000580	0.002300	0.001470
Rank	3	1	2

The Taguchi method converts the experimental findings into a signal-to-noise (S/N) ratio shown in Table 3. The investigation of the specific wear rate of the Al7075 composite (Reinforced by 3%, 6%, and 9% weight) led to the adoption of the lower-the-better quality characteristic in this study. The S/N analysis was used to calculate the S/N ratio for every process parameter level shown in Table 4.

Using the Minitab software, an investigation of the impact of each control factor (A, B, and C) on the particular wear rate was carried out using a S/N response table. The response of the specific wear rate is shown in Table 5. It directs the S/N ratio at each level of the control factor and in what way it changed when the settings of each control factor were changed from levels 1 to 3. Various values were used to identify which control factor had the most influence. It can be observed from the results that the strongest influence was exerted by the applied load and the Sliding speed, respectively. The effect of the Sliding speed was stronger than the Material type (Reinforcement Added).

This behavior aligns well with the findings. Figures 5 (a) and (b) show the main effect plots for the specific wear rate of the Fe₃O₄-reinforced Al7075 composite for the S/N ratio and mean value, respectively. Optimal testing conditions of these control factors could be very easily determined from the response graphs. It could be observed from Table 4 that the initial optimum condition for the tested samples becomes A3B1C1 for the main control factors. It was evident that Al7075 + 9% Fe₃O₄ composite material had the greatest effect on the optimal testing condition.

Analysis of Variance (ANOVA)

The importance of factors influencing the responses, such as wear rate, is assessed using analysis of variance (ANOVA). ANOVA is often performed with great accuracy at a 95% confidence level and 5% significance. A value for



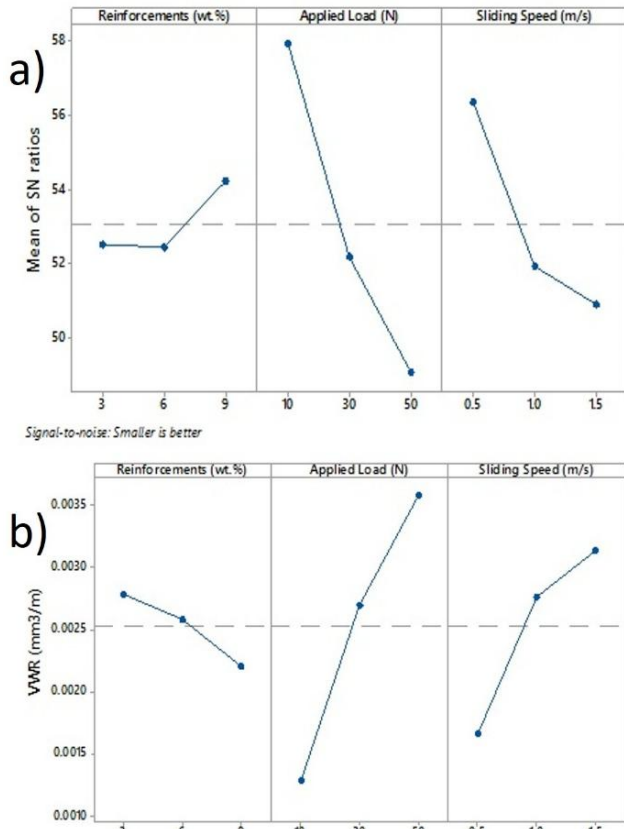


Figure 5. Main effect plots for wear rate of Al7075 composite (Reinforced by 3%, 6%, and 9% wt.); a) S/N ratio, and b) Means.

P under 0.05 implies a larger influence on wear rate. The P stands for the significance of each parameter. The parameters, as shown in Table 6, are taken into account for evaluating the percentage contribution of each parameter to the wear rate.

Confirmation test

Appropriate confirmation tests were conducted to verify the regression equation based on the ANOVA-determined significance of the parameters. The confirmation test u (1) model developed with the cumulative effect coming f control parameters in wear rate and coefficient of friction, as provided in equation (1)

$$10^5 VWR = -9.2 - 9.7 \text{ Reinforcement} + 5.7 \text{ Applied Load} + 147.0 \text{ Sliding Speed}$$

Model Summary:

$$S = 0.0004243; R\text{-sq} = 92.84\%; R\text{-sq(adj)} = 88.55\%$$

Figure 6 demonstrates that across all speed ranges, there is a significant interaction between the reinforcement and speed on the wear rate. This effect was evident at high speeds because higher reinforcement weight percentages typically provide greater resistance to wear as speed increases and ploughing eventually occurs, resulting in greater material removal.

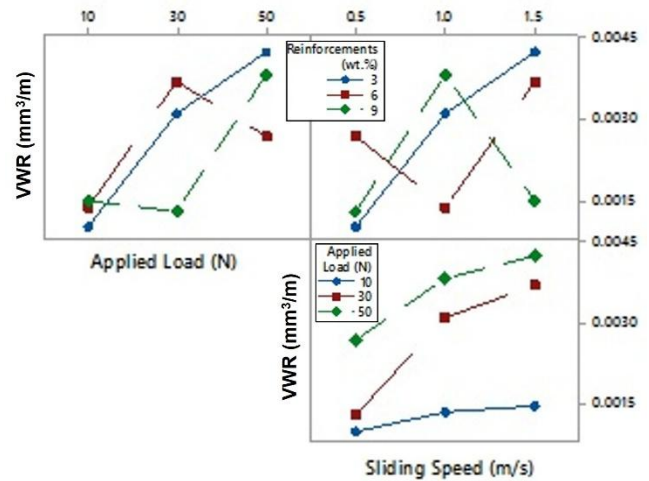


Figure 6. Interaction Plot for VWR.

It can be seen in Table 6 results that F-values were computed statistically, and the percentage of reinforcement (wt%), applied load (N), and sliding distance (m) were input process factors. ANOVA revealed that weight, in terms of the percentage of reinforcement (1.08%), wear rate, sliding distance (7.27%), and applied load (16.73%) were significant factors.

Table 6. Analysis of Variance for wear rate (mm³/m).

Source	Reinforcement	Applied Load	Sliding Speed	Error	Total
DF	2	2	2	2	8
Adj SS	0.000001	0.000008	0.000004	0	1.3E-5
Adj MS	0	0.000004	0.000002	0	
F-Value	1.08	16.73	7.27		
P-Value	0.481	0.056	0.0121		
%Contribution	7.6923	61.53	30.769	0	100
Remark	Insignificant	Significant	Significant		

Model Summary:

$$S = 0.0004911; R\text{-sq} = 96.17\%; R\text{-sq(adj)} = 84.66\%$$

Table 7. Factor Levels and wear rate (mm³/m) for Predictions.

Reinforcements (wt%)	3
Applied Load (N)	10
Sliding Speed (m/s)	0.5
S/N Ratio	60.6684
Mean (VWR mm ³ /m)	0.00069

Table 7 shows the predicted factor levels for optimum combinations of reinforcement, applied load and sliding speed. For 3%wt Reinforcement of Fe₃O₄, at a load of 10 N and 0.5 m/s sliding speed, a significant value of the wear results is expected. Also, Table 7 presents the predicted and experimentally determined values for wear rate designed for different combinations of affecting parameters.

Usually, sliding speed has less impact on the particular wear rate of Metal Matrix Composites than does applied load. In comparison to Al7075 + 3% Fe₃O₄ under the same test conditions, the average specific wear rates for Al7075 + 6% Fe₃O₄ and Al7075 + 9% Fe₃O₄ composites are approximately 37% and 10% lower, respectively.

Surface Morphology Analysis

The worn surfaces of aluminum composites (provided for an applied load of 50 N) regularly showed grooves of varying diameters in Figure 7(a)–(c). Numerous times, the structure of these grooves created by the sliding of aluminum composites has been connected to the delamination process, which is the preferential spread of subsurface cracks along the sliding direction that results in the detachment of wear particles in the form of sheets or flakes [15]. As a result of ceramic particles stuck at the sliding contact and standing proud of the composite sample's worn surface, visible grooves also served as proof of abrasive operations during sliding.

In Figure 7(c), when the Fe₃O₄ particles protrude above the sliding surface, the load on the Al7075 + 9% Fe₃O₄ composite surface could primarily be supported by the Fe₃O₄ particles. Consequently, friction would primarily have taken place between the particles and the surface of the stainless-steel disc. Adhesive wear would have also taken place since the composite surface, due to material transport, is no longer coated with Fe₃O₄ particles.

The mechanism of friction occurred between the two metal surfaces. In this connection, the rigid Fe₃O₄ particles can be detached from the aluminum composite surface alongside debris that includes Fe₃O₄ particles, owing to the development of fatigue cracks in the matrix below the aluminum composite surface.

The surface of the Al7075 alloy demonstrated deep grooves, debris, delamination, and signs of severe adhesive wear, according to the SEM pictures. The process by which asperities on contacting surfaces fuse under pressure and friction is known as adhesive wear. These welds fracture with continued relative motion, causing material to rip and be removed from both sides. Scratching and material removal can also be facilitated by abrasive particles becoming trapped between the contacting surfaces. Deep abrasive grooves were formed mostly by Fe₃O₄ particles in the composites, according to the SEM examination of the worn surfaces. Additionally, these particles might have prevented material pieces from separating during wear, which could have resulted in delamination.

Conclusions

The research focused on improving how long aluminum alloy (Al7075) can last and perform better, especially by making it more resistant to wear (surface damage caused by friction). To achieve this, iron oxide (Fe₃O₄) particles were added to the aluminum alloy, and the mixture was made using the stir casting process, which ensures even distribution of the reinforcement particles.

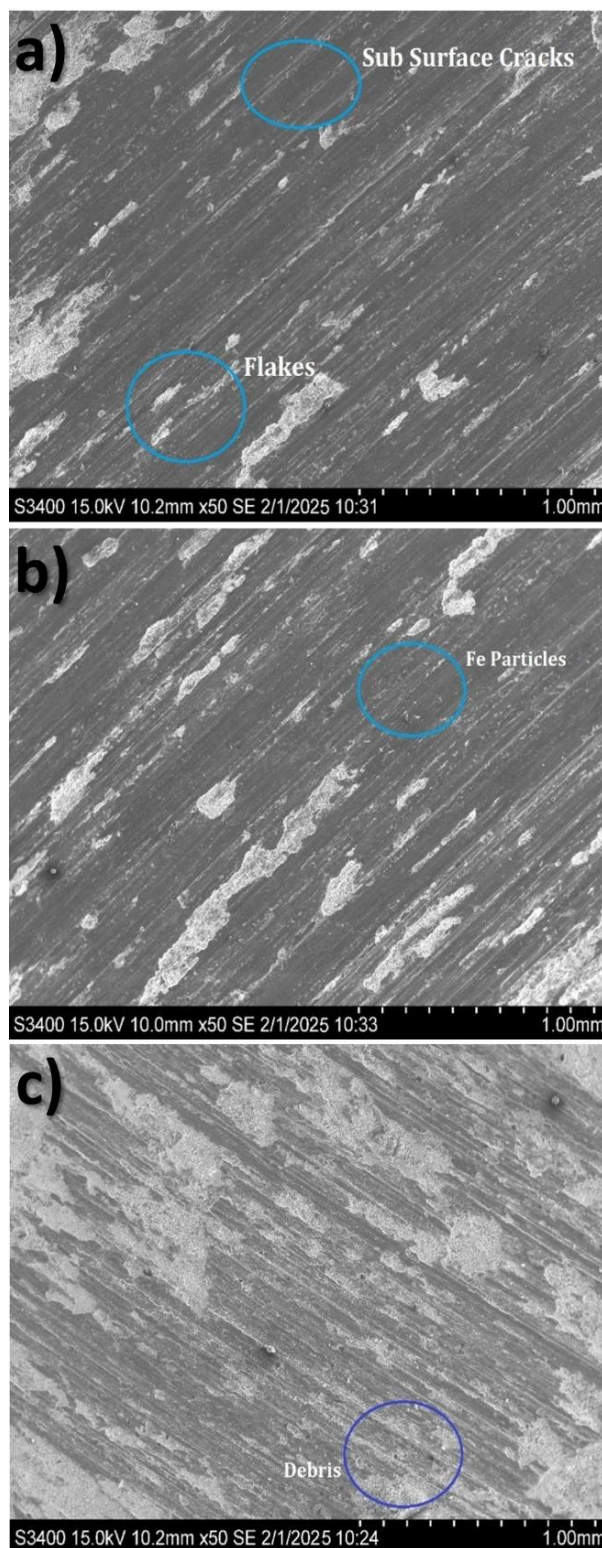


Figure 7. The SEM microstructure of worn specimens of (a) Al7075 + 3% Fe₃O₄, (b) Al7075 + 6% Fe₃O₄, (c) Al7075 + 9% Fe₃O₄.

Using Taguchi's method, the study found the best combination of process parameters to minimize wear. The best results were obtained when the load was 10 newtons, the reinforcement content was 3% Fe₃O₄, and the sliding speed was 0.5 m/s.

The ANOVA (Analysis of Variance) results showed that the load was the most important factor influencing wear loss, contributing about 61.5% of the effect, while sliding velocity was the next most important (about 30.8%). In general, as both load and speed increased, wear also increased.

The addition of Fe₃O₄ helped make the composite material stronger and tougher, due to better particle dispersion and finer grain size in the aluminum matrix. The main wear mechanism observed was adhesive wear, which happens when material from one surface sticks and transfers to another during sliding. The Fe₃O₄ particles helped resist this effect and reduced the surface damage.

Finally, when more Fe₃O₄ particles were added, the specific wear rate (SWR) decreased, meaning the material became more wear-resistant. This improvement was due to the uniform distribution of the hard Fe₃O₄ particles, which increased the hardness of the composite and helped it resist scratches and cuts from the counter surface during sliding.

The development and optimization of aluminum base composites in a range of industrial applications will be significantly impacted by the study's conclusions. The Al7075 + Fe₃O₄ composites' improved wear resistance and frictional properties indicate their potential usage in high-stress sectors such as automotive, aerospace, and manufacturing, where material durability is crucial.

Optimal reinforcement and process parameter combinations can reduce wear and friction, resulting in longer-lasting components and increased system reliability. Furthermore, the potential of these advanced statistics in materials engineering is demonstrated by the effective use of the Taguchi method and ANOVA predictions. In conclusion, this study emphasizes the usefulness and industrial significance of these materials in addition to advancing the

comprehension of the tribological behavior of Al7075 + Fe₃O₄ composites.

Acknowledgements

The authors gratefully acknowledge the support from the Sai Vidya Institute of Technology and Ballari Institute of Technology and Management, Ballari.

References

- [1]. G.E. Kiourtsidis, S.M. Skolianos, *Wear* **253**, 946 (2002).
- [2]. M. Muratoğlu, M. Aksoy, *Mater. Sci. Eng. A* **282**, 91 (2000).
- [3]. P.H. Shipway, A.R. Kennedy, A.J. Wilkes, *Wear* **216**, 160 (1998).
- [4]. S.C. Lim, M. Gupta, L. Ren, J.K.M. Kwok, *Mater. Process. Technol.* **89-90**, 591 (1999).
- [5]. Y. Sahin, *Mater. Des.* **24**, 95 (2003).
- [6]. D.P. Mondal, S. Das, A.K. Jha, A.H. Yegneswaran, *Wear* **223**, 131 (1998).
- [7]. A. Shivaramakrishna, R. Subramanya, Y. Basavaraj, *Adv. Mater. Process. Technol.* **8**, 4598 (2022).
- [8]. B.M. Gopalsamy, B. Mondal, S. Ghosh, *Int. J. Adv. Manuf. Technol.* **43**, 237 (2009).
- [9]. A. Shivaramakrishna, Y. Basavaraj, R. Subramanya, *Int. J. Cast Met. Res.* **35**, 51 (2022).
- [10]. G. Straffelini, C. Giuliani, M. Pellizzari, E. Veneri, M. Bronzato, *Wear* **271**, 1602 (2011).
- [11]. F.H. Stott, *Tribol. Int.* **31**, 61 (1998).
- [12]. J. Zhang, A.T. Alpas, *Acta Mater.* **45**, 513 (1997).
- [13]. M.A. Chowdhury, M.K. Khalil, D.M. Nuruzzaman, M.L. Rahaman, *Int. J. Mech. Mechatron. Eng.* **11**, 53 (2011).
- [14]. R.A. Al-Samarai, Haftirman, K.R. Ahmad, Y. Al-Douri, *Int. J. Sci. Res. Publications* **2**(3), 37 (2012).
- [15]. D. Nagesh, S. Raghavendra, N.M. Sivaram, S. Suresh, B. Manjunatha, S. Sanketh, *Adv. Mater. Process. Technol.* **8**, 3248 (2021).